IEEE Access
Multidisciplinary | Rapid Review | Open Access Journal

SPECIAL SECTION ON 5G AND BEYOND MOBILE WIRELESS COMMUNICATIONS ENABLING INTELLIGENT MOBILITY

Received August 7, 2019, accepted August 21, 2019, date of publication August 26, 2019, date of current version September 5, 2019.

Digital Object Identifier 10.1109/ACCESS.2019.2937470

Performance Analysis of One-Way Highway Vehicular Networks With Dynamic Multiplexing of eMBB and URLLC Traffics

XIAOSHI SONG, (Member, IEEE), AND MENGYING YUAN
[1]School of Computer Science and Engineering, Northeastern University, Shenyang 110819, China
[2]Engineering Research Center of Security Technology of Complex Network System, Ministry of Education, Northeastern University, Shenyang 110819, China

Corresponding author: Xiaoshi Song (songxiaoshi@cse.neu.edu.cn)

This work was supported in part by the NSFC under Grant 61701102, Grant 61871107, Grant 61701100, and Grant 61671141, in part by the Fundamental Research Funds for the Central Universities under Grant N181604005, in part by the National Key Research and Development Program of China under Grant 2018YFB1702000, and in part by the Fundamental Research Funds for the Central Universities under Grant N180716019.

ABSTRACT The services of enhanced mobile broadband (eMBB) and the ultra-reliable low-latency communication (URLLC) enabled by 5G new radio (NR) are considered as the essential prerequisites of the future intelligent transportation systems. Particularly, the eMBB service is designed to provide extremely high data rate for content delivery and thereby can significantly enhance the quality of experience (QoE) of the bandwidth-hungry in-vehicle entertainment applications. On the other hand, the URLLC is designed to tackle the stringent requirements on the latency and reliability of the critical packets transmissions, and thereby can facilitate the autonomous driving of the connected vehicles. In this paper, under the scenario of a one-way highway vehicular network, we address the issue of joint resource allocations of the eMBB and URLLC traffics for the enhancement of the network performance. The eMBB traffic is assumed to be full-buffered and scheduled at the boundary of each time slot for multimedia transmissions. During each eMBB transmission interval, random arrivals of URLLC traffics are assumed. To satisfy the latency constraint of the URLLC transmissions, the eMBB time slot is divided into minislots and the newly arrived URLLC traffic is promptly scheduled in the next minislot by puncturing the on-going eMBB traffics. Further, to guarantee the reliability of the URLLC traffic, guard zones are deployed around the vehicle receivers as protections and the eMBB transmissions inside the guard zones are prohibited. Under this context, we first derive the transmission probability of the RSU nodes. Then, based on the obtained results, we capture association probabilities of the vehicle receivers for URLLC and eMBB traffics, respectively. Finally, the coverage performance of the vehicle-to-vehicle (V2V) links and the rate coverage performance of the vehicle-to-infrastructure (V2I) links are analyzed.

INDEX TERMS Vehicular networks, eMBB, URLLC, stochastic geometry, minislots, puncturing, coverage probability, rate coverage probability.

I. INTRODUCTION

The recent achievements of autonomous driving and enormous demands for the more efficient traffic management have boosted the development of the intelligent transport system (ITS) [1]–[6]. One of the major technical challenges in the design of ITS is how to effectively coordinate the connected vehicles and share the safety-critical or bandwidth-intensive messages. Among various techniques, the emerging 5G based vehicle-to-everything (V2X) communication, which includes the vehicle-to-vehicle (V2V) and vehicle-to-infrastructure (V2I) communication modes, has been considered as a promising solution and attracted great attention in both academia and industries [7]–[14]. It is envisioned that the use of the V2X communication can significantly enhance the performance of the future ITS by enabling more advanced vehicle networking strategies and data exchanging policies.

The associate editor coordinating the review of this article and approving it for publication was Ke Guan.

The enhanced mobile broadband (eMBB) and the ultra-reliable low-latency communication (URLLC) empowered by the 5G new radio are considered as the key features of the V2X technology. Particularly, the eMBB service is designed to accommodate the massive data transmissions induced by the in-vehicle entertainment applications, while the URLLC is designed to guarantee the delivery of critical road safety information. In literature, dynamic multiplexing of eMBB and URLLC traffics has been considered by several works under the 5G scenario [15]–[24]. In [15], Wu *et al.* incorporated the signal space diversity scheme into the dynamical puncturing scheme for the dynamic downlink multiplexing of eMBB and URLLC traffics. In [16], Anand *et al.* considered the optimal online joint scheduling of the eMBB and URLLC transmissions to maximize the eMBB utility while guarantee the URLLC requirements. In [17], Park *et al.* investigated the downlink URLLC-eMBB slicing for the transmissions of the virtual reality traffics. In [18], Kassab *et al.* studied the coexistence of URLLC and eMBB services in the C-RAN uplink based on orthogonal multiple access and non-orthogonal multiple access techniques, and provided the information theoretic analysis of the respective tradeoffs. In [19], Esswie *et al.* proposed a novel null-space-based preemptive scheduling strategy to grant the URLLC traffic with a higher priority while achieve the best possible eMBB data rate. Further, in [20], an enhanced null-space-based preemptive scheduling strategy was developed with a significantly improved ergodic capacity. In [21], Tang *et al.* considered the incorporations of multiple eMBB and URLLCslices in C-RAN for the maximization of the operator's revenue. In [22], Zhang *et al.* employed machine learning into the joint scheduling of the eMBB and uRLLC traffics in 5G networks. In [23], a risk-sensitive based joint scheduling strategy is considered for eMBB and URLLC transmissions. Further, in [24], the resource scheduling problem of URLLC and eMBB traffics was addressed by applying a 2-Dimensions Hopfield Neural Network. It is worth noting that though the efforts on the design of joint scheduling of the eMBB and uRLLC traffics have been made in the existing works, none of them considered the V2X scenario.

Different from [15]–[24], in this paper, we analyze the performance of the joint scheduling of eMBB and URLLC traffics in vehicular network by applying tools from stochastic geometry. The main contributions of this paper are summarized as follows:

- We consider a one-way highway vehicular network with the locations of the vehicle nodes and road side unit (RSU) nodes modeled as 1D Poisson point processes (PPPs) on a straight line of infinite length. The eMBB traffic is assumed to be full-buffered and scheduled at the boundary of each time slot for multimedia transmissions. During each eMBB transmission interval, random arrivals of URLLC traffics are assumed. To satisfy the latency constraint of the URLLC transmissions, the eMBB time slot is divided into minislots and the newly arrived URLLC traffic is promptly scheduled in the next minislot by puncturing the on-going eMBB traffics. Further, to guarantee the reliability of the URLLC traffic, guard zones are deployed around the vehicle receivers as protections and the eMBB transmission inside the guard zones are prohibited.
- The transmission probability of RSU nodes is derived. Then, based on the obtained result, the association probabilities of the vehicle receivers for URLLC and eMBB traffics are derived and analyzed, respectively. Finally, the coverage performance of the V2V links, i.e., the URLLC transmission, and the rate coverage performance of the V2I links, i.e., the eMBB transmissions, are characterized. We confirm our analysis and discuss the impact of the key network parameters on the joint scheduling of the URLLC and eMBB traffics through extensive simulations. We also compare the proposed guard-zone based URLLC scheduling policy with the baseline policy where the guard zone around vehicle receiver is not applied, and demonstrate the superiority.

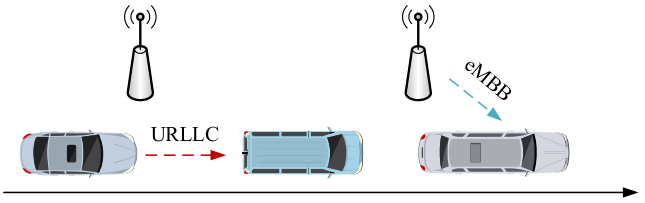

FIGURE 1. One-way highway vehicular network with vehicle nodes and RSU nodes.

The remainder of this paper is organized as follows. In Section II, we describe mathematical model of the one-way highway vehicular network and present guard-zone based URLLC scheduling policy. In Section III, we calculate two kinds of association probabilities of the vehicle receivers, i.e., the probability that a vehicle receiver is associated with the respective vehicle transmitter for URLLC transmission, and the probability that a vehicle receiver is associated with the nearest RSU node for eMBB transmission. In Section IV, we derive the coverage probabilities of the V2V links, i.e., the URLLC transmission, and the rate coverage performance of the V2I links, i.e., the eMBB transmissions, respectively. Section V confirms the credibility of our analysis and compares the performance with the baseline strategy through numerical simulations. Finally, the conclusions are drawn in Section VI. Notations of selected symbols used in this paper are summarized in Table 1.

II. SYSTEM MODEL

A one-way highway vehicular network is considered, where the vehicles and RSU nodes are assumed to be randomly distributed and occupy the same frequency resource on an infinite line as illustrated in Fig. 1. Particularly, the vehicle receivers are modeled as 1D homogeneous Poisson point processes with density λ_v. Further, it is assumed that for each vehicle receiver, its potentially associated vehicle transmitter is located at a fixed distance of d_v. As such, the vehicle transmitters follow a 1D homogeneous Poisson point processes

TABLE 1. Symbol notation.

Symbol	Meaning
λ_r, λ_v	Density of RSUs, V2Vs
W	Bandwidth of system
K	Load of a RSU node
α	Path-loss exponent
P_r	Transmit power of RSU node
P_v	Transmit power of vehicle transmitters
$\mathcal{T}$	Rate target for eMBB traffic
θ	SIR target for URLLC traffic
p	Arrival probability of URLLC traffic
R_d	The radius of guard zone
ς_r^a	Transmission probability of RSU node
ζ_v^t	The probability that a vehicle receiver is associated with its paired vehicle transmitter
ζ_r	The probability that a vehicle receiver is associated with its nearest active RSU
ζ_a	The activation probability of vehicle receivers in the Voronoi cell of active RSU nodes
$\overline{N}$	Mean load of RSU nodes
l	The size of Voronoi cell
d	The distance between a vehicle receiver and its nearest RSU
Π_r^t, Π_v^a	Point process formed by the active RSUs, vehicle transmitters
λ_r^a, λ_v^a	Density of active RSUs, vehicle transmitters
$\mathcal{C}_v$	Coverage probability of a vehicle receiver which associates with its paired vehicle transmitter
$\mathcal{C}_d^r$	Conditional rate coverage probability $\mathcal{C}_d^r$ of vehicle receiver which associates with a RSU node for eMBB traffics at a distance of d away
$\mathcal{C}_r$	Rate coverage probability of a vehicle receiver which associates with its nearest RSU

with density λ_v. The RSU nodes are assumed to follow 1D homogeneous Poisson point processes with density λ_r which is independent from the vehicle nodes.

The transmit powers of vehicle nodes and RSU nodes are assumed to be P_v and P_r, respectively. The channel gain of small-scale fading is assumed to be independent and exponentially distributed (Rayleigh fading) with unit mean. Further, the pathloss is defined as $d^{-\alpha}$ for distance d and path-loss exponent α.

The vehicle receivers are assumed to be associated with the nearest RSU node by default for eMBB transmissions. Particularly, the eMBB traffics are assumed to be full-buffered and scheduled at the boundary of each time slot. During each eMBB transmission interval, random arrivals of URLLC traffics generated at the vehicle transmitters are assumed. To satisfy the latency constraint of the URLLC transmissions, the eMBB time slot is divided into M minislots and the newly arrived URLLC traffic is promptly scheduled in the next minislot by puncturing the on-going eMBB traffics. We assume that for each Voronoi cell, the URLLC traffic arrives at a randomly selected vehicle transmitter in each minislot with probability p. Then, if the URLLC traffic is scheduled at a vehicle transmitter, its paired vehicle receiver stops communicating with the nearest RSU node and starts to receive the URLLC messages. Further, to guarantee the reliability of the URLLC traffic, guard zones with radius R_d are deployed around the vehicle receivers which receive the URLLC messages as protections and the eMBB transmissions inside the guard zones are prohibited.

III. ASSOCIATION PROBABILITY

In this section, we characterize the association probability of the vehicle receivers for URLLC and eMBB traffics, respectively. Particularly, let λ_v^a denote the density of the active vehicle transmitters. We first characterize λ_v^a in the following lemma.

Lemma 1: For the studied one-way highway vehicular network, under the proposed guard-zone based URLLC scheduling policy, the density λ_v^a of the active vehicle transmitters is given by

$$\lambda_v^a = \lambda_r(1 - e^{-\frac{\lambda_v}{\lambda_r}}) \cdot p. \tag{1}$$

Proof: It can be easily verified that the average number of vehicle transmitters in each Voronoi cell of RSU nodes is $\frac{\lambda_v}{\lambda_r}$. Then, the probability that there is at least one vehicle transmitter in the tagged Voronoi cell is given by $1 - e^{-\frac{\lambda_v}{\lambda_r}}$. Further, by noting that for each Voronoi cell, the URLLC traffic arrives at a randomly selected vehicle transmitter in each minislot with probability p, (1) is immediately obtained. □

Let ς_r^a denote the transmission probability of RSU nodes. Then, with the obtained result of λ_v^a, we derive ς_r^a in the following lemma.

Lemma 2: For the studied one-way highway vehicular network, under the proposed guard-zone based URLLC scheduling policy, the transmission probability ς_r^a of RSU nodes is given by

$$\varsigma_r^a = (1 - e^{-\frac{\lambda_v}{\lambda_r}}) \cdot e^{-2\lambda_r(1-e^{-\frac{\lambda_v}{\lambda_r}})p \cdot R_d}, \tag{2}$$

Proof: Under the proposed guard-zone based URLLC scheduling policy, by noting that $\varsigma_r^a = (1 - e^{-\frac{\lambda_v}{\lambda_r}}) \cdot e^{-2\lambda_v^a R_d}$, (2) is immediately obtained based on Lemma 1. □

Let λ_r^a denote the density of active RSUs. Then, we obtain the following corollary.

Corollary 1: For the studied one-way highway vehicular network, under the proposed guard-zone based URLLC scheduling policy, the density λ_r^a of active RSU nodes is given by

$$\lambda_r^a = \lambda_r(1 - e^{-\frac{\lambda_v}{\lambda_r}}) \cdot e^{-2\lambda_r(1-e^{-\frac{\lambda_v}{\lambda_r}})p \cdot R_d}. \tag{3}$$

Proof: Under the proposed guard-zone based URLLC scheduling policy, it can be easily verified that $\lambda_r^a = \lambda_r \varsigma_r^a$, which thereby completes the proof. □

It is worth noting that under the proposed guard-zone based URLLC scheduling policy, the vehicle receivers can be categorized into two different kinds, i.e., the vehicle receivers associated with the vehicle transmitters for URLLC traffics, and the vehicle receivers associated with the nearest RSU for eMBB traffics, respectively. Particularly, for a vehicle receiver, we denote ζ_v^t as the probability a vehicle receiver is associated with its paired vehicle transmitter. Further, we denote ζ_r as the probability the a vehicle receiver is associated with its nearest active RSU node. Then, in the following two lemmas, we characterize ζ_v^t and ζ_r, respectively.

Lemma 3: For the studied one-way highway vehicular network, under the proposed guard-zone based URLLC scheduling policy, the association probability ζ_v^t of vehicle receivers with respect to their paired vehicle transmitters for URLLC traffics is given by

$$\zeta_v^t = \frac{\lambda_r(1-e^{-\frac{\lambda_v}{\lambda_r}})\cdot p}{\lambda_v}. \tag{4}$$

Proof: By noting that

$$\begin{aligned}\lambda_v^a &= \lambda_v \zeta_v^t \\ &= \lambda_r(1-e^{-\frac{\lambda_v}{\lambda_r}})\cdot p.\end{aligned} \tag{5}$$

ζ_v^t can be immediately obtained based on Lemma 1. □

Lemma 4: For the studied one-way highway vehicular network, under the proposed guard-zone based URLLC scheduling policy, the association probability ζ_r of vehicle receivers with respect to their nearest RSU nodes for eMBB traffics is given by

$$\zeta_r = \left(1-e^{-\frac{\lambda_v}{\lambda_r}}\right)e^{-2\lambda_r(1-e^{-\frac{\lambda_v}{\lambda_r}})pR_d}\left(1-\frac{\lambda_r}{\lambda_v}p\right). \tag{6}$$

Proof: Let ζ_a denote the activation probability of vehicle receivers in the Voronoi cell of active RSU nodes. It can be easily obtained that

$$\begin{aligned}\lambda_v\zeta_a &= \lambda_r^a \cdot \frac{\lambda_v}{\lambda_r} \\ &= \lambda_r(1-e^{-\frac{\lambda_v}{\lambda_r}})\cdot e^{-2\lambda_r(1-e^{-\frac{\lambda_v}{\lambda_r}})pR_d}\cdot\frac{\lambda_v}{\lambda_r} \\ &= \lambda_v(1-e^{-\frac{\lambda_v}{\lambda_r}})\cdot e^{-2\lambda_r(1-e^{-\frac{\lambda_v}{\lambda_r}})pR_d}.\end{aligned} \tag{7}$$

It is noting that in the Voronoi cell of active RSU nodes, the vehicle receivers may either associate with the tagged RSU nodes or with their paired vehicle transmitter. As such, we have the following equality on the density of active vehicle receivers associated with the RSU nodes as

$$\begin{aligned}\lambda_v\zeta_r &= \lambda_v\zeta_a - \lambda_r^a\cdot p \\ &= \lambda_v(1-e^{-\frac{\lambda_v}{\lambda_r}})\cdot e^{-2\lambda_r(1-e^{-\frac{\lambda_v}{\lambda_r}})pR_d} \\ &\quad -\lambda_r(1-e^{-\frac{\lambda_v}{\lambda_r}})e^{-2\lambda_r(1-e^{-\frac{\lambda_v}{\lambda_r}})pR_d}\cdot p \\ &= \left(1-e^{-\frac{\lambda_v}{\lambda_r}}\right)e^{-2\lambda_r(1-e^{-\frac{\lambda_v}{\lambda_r}})pR_d}(\lambda_v-\lambda_r p),\end{aligned} \tag{8}$$

where ζ_r is immediately obtained. □

IV. NETWORK PERFORMANCE

We are now ready to analyze the performance of one-way highway vehicular network with the proposed guard-zone based URLLC scheduling policy. We first characterize the coverage probability $\mathcal{C}_v$ of vehicle receivers associated with their paired transmitters for URLLC traffics in the following lemma.

Theorem 1: For the studied one-way highway vehicular network, under the proposed guard-zone based URLLC scheduling policy, the coverage probability $\mathcal{C}_v$ of vehicle receivers which associate with their paired transmitters for URLLC traffics is given by

$$\mathcal{C}_v = \exp\left\{-2\left(\eta + \int_{R_d}^{\infty}\varpi(d_r)\mathrm{d}d_r + \varrho\right)\right\}, \tag{9}$$

where η, $\varpi(d_r)$, ϱ are given as

$$\begin{aligned}\eta = &\frac{\theta P_r {d_v}^{\alpha}}{(-1+\alpha)P_v}\left(1-e^{-\frac{\lambda_v}{\lambda_r}}\right) \\ &\times(1-e^{-2R_d\lambda_r(1-e^{-\frac{\lambda_v}{\lambda_r}})e^{-2\lambda_r(1-e^{-\frac{\lambda_v}{\lambda_r}})pR_d}}) \\ &\times e^{-2R_d\lambda_r(1-e^{-\frac{\lambda_v}{\lambda_r}})p}{\lambda_r}{R_d}^{1-\alpha} \\ &\times{}_2\mathrm{F}_1\left[1,\frac{-1+\alpha}{\alpha},2-\frac{1}{\alpha},-\frac{\theta P_r\left(\frac{d_v}{R_d}\right)^{\alpha}}{P_v}\right],\end{aligned} \tag{10}$$

$$\begin{aligned}\varpi(d_r) = &\frac{P_r\theta {d_r}^{1-\alpha}}{(-1+\alpha)P_v}\left(1-e^{-\frac{\lambda_v}{\lambda_r}}\right)^2{d_v}^{\alpha} \\ &\times e^{-2(\lambda_r(1-e^{-\frac{\lambda_v}{\lambda_r}})e^{-2\lambda_r(1-e^{-\frac{\lambda_v}{\lambda_r}})pR_d}d_r)} \\ &\times 2\,e^{-4\lambda_r(1-e^{-\frac{\lambda_v}{\lambda_r}})pR_d}\,{\lambda_r}^2 \\ &{}_2\mathrm{F}_1\left[1,\frac{-1+\alpha}{\alpha},2-\frac{1}{\alpha},-\frac{\theta P_r\left(\frac{d_v}{d_r}\right)^{\alpha}}{P_v}\right],\end{aligned} \tag{11}$$

and

$$\varrho = \frac{\left(1-e^{-\frac{\lambda_v}{\lambda_r}}\right)\lambda_r p\pi d_v\theta^{\frac{1}{\alpha}}\csc\left(\frac{\pi}{\alpha}\right)}{\alpha}, \tag{12}$$

respectively, with d_r denoting the distance between the tagged vehicle receiver and its nearest active RSU node, and ${}_2\mathrm{F}_1(a,b;c;z)$ denoting the hypergeometric function of parameter a, b, c, z as

$${}_2\mathrm{F}_1(a,b;c;z) = \sum_{n=0}^{\infty}\frac{(a)_n(b)_n}{(c)_n}\frac{z^n}{n!}, \tag{13}$$

and $(q)_n$ denoting the Pochhammer symbol as

$$(q)_n = \begin{cases}1, & n=0, \\ q(q+1)\cdots(q+n-1), & n>0.\end{cases} \tag{14}$$

Proof: See Appendix A. □

We next characterize the rate coverage probability $\mathcal{C}_r$ of the vehicle receivers associated with their nearest RSU nodes for eMBB traffics. Particularly, we first derive the conditional rate coverage probability $\mathcal{C}_d^r$ of vehicle receiver which associates with a RSU node for eMBB traffics at a distance of d away in the following lemma.

Lemma 5: For the studied one-way highway vehicular network, under the proposed guard-zone based URLLC scheduling policy, the conditional rate coverage probability $\mathcal{C}_d^r$ of vehicle receiver which associates with a RSU node for eMBB traffics at a distance of d away is given by

$$\mathcal{C}_d^r = \sum_{k=0}^{\infty}\exp\left\{-2\left(\xi+\int_{2R_d}^{\infty}\varphi(l)\mathrm{d}l+\vartheta\right)\right\}\frac{\left(\frac{\lambda_v}{\lambda_r}\right)^k}{k!}e^{-\frac{\lambda_v}{\lambda_r}}, \tag{15}$$

where ξ, $\varphi(l)$, ϑ are given as

$$\xi = -\frac{\left(-1+2^{\frac{\mathcal{T}(K+1)}{W}}\right)}{(-1+\alpha)} e^{-4\,R_d\lambda_r(1-e^{-\frac{\lambda_v}{\lambda_r}})e^{-2\lambda_r(1-e^{-\frac{\lambda_v}{\lambda_r}})pR_d}} \times\Bigg(1-e^{4\,R_d\lambda_r(1-e^{-\frac{\lambda_v}{\lambda_r}})e^{-2\lambda_r(1-e^{-\frac{\lambda_v}{\lambda_r}})pR_d} + 4\,R_d\lambda_r(1-e^{-\frac{\lambda_v}{\lambda_r}})e^{-2\lambda_r(1-e^{-\frac{\lambda_v}{\lambda_r}})pR_d}\Bigg)\left(\frac{d}{R_d}\right)^{\alpha} R_d \times {}_2\mathrm{F}_1\left[1,\frac{-1+\alpha}{\alpha},2-\frac{1}{\alpha},\left(1-2^{\frac{\mathcal{T}(K+1)}{W}}\right)\left(\frac{d}{R_d}\right)^{\alpha}\right], \tag{16}$$

$$\varphi(l) = \frac{2^{\alpha+1}\left(-1+2^{\frac{\mathcal{T}(K+1)}{W}}\right)}{(-1+\alpha)} d^{\alpha} l^{2-\alpha} \times\left(\lambda_r(1-e^{-\frac{\lambda_v}{\lambda_r}})\cdot e^{-2\lambda_r(1-e^{-\frac{\lambda_v}{\lambda_r}})pR_d}\right)^2 \times {}_2\mathrm{F}_1\left[1,\frac{-1+\alpha}{\alpha},2-\frac{1}{\alpha},\left(1-2^{\frac{\mathcal{T}(K+1)}{W}}\right)\left(\frac{2d}{l}\right)^{\alpha}\right] \times e^{-2l\lambda_r(1-e^{-\frac{\lambda_v}{\lambda_r}})\cdot e^{-2\lambda_r(1-e^{-\frac{\lambda_v}{\lambda_r}})pR_d}}, \tag{17}$$

and

$$\vartheta = \lambda_r\left(1-e^{-\frac{\lambda_v}{\lambda_r}}\right)p\pi\left(\frac{d^{-\alpha}P_v}{\left(-1+2^{\frac{\mathcal{T}(K+1)}{W}}\right)P_r}\right)^{-\frac{1}{\alpha}}\frac{\csc(\frac{\pi}{\alpha})}{\alpha}, \tag{18}$$

respectively, with l denoting the size of the active Voronoi cell.

Proof: See Appendix B. □

Based on Lemma 5, we obtain the following theorem.

Theorem 2: For one-way highway vehicular networks, under the proposed guard-zone based URLLC scheduling policy, the rate coverage probability $\mathcal{C}_r$ of vehicle receivers which associate with the nearest RSU node for eMBB traffics is given by

$$\mathcal{C}_r = \int_0^{\infty}\sum_{K=0}^{\infty}\exp\left\{-2\left(\xi+\int_{2R_d}^{\infty}\varphi(l)\mathrm{d}l+\vartheta\right)\right\} \times\frac{(\frac{\lambda_v}{\lambda_r})^K}{K!}e^{-\frac{\lambda_v}{\lambda_r}}\cdot 2\lambda_r e^{-2\lambda_r d}\mathrm{d}d, \tag{19}$$

where ξ, $\varphi(l)$, ϑ is given by (16), (17), (18), respectively.

Proof: By noting that $\mathcal{C}_r = \int_0^{\infty}\mathcal{C}_d\cdot 2\lambda_r e^{-2\lambda_r d}\mathrm{d}d$, (19) is immediately obtained. □

V. NUMERICAL RESULTS

In this section, we simulate the one-way highway vehicular network under the proposed guard-zone based URLLC scheduling policy to validate our analysis. Particularly, Monte Carlo method is applied and the simulations are performed on a line of 1000m. The density of the vehicle receivers is set to be $\lambda_v = 1$. The transmit power of the RSU is set to be $P_r = 3$W, and the transmit power of the vehicle transmitters

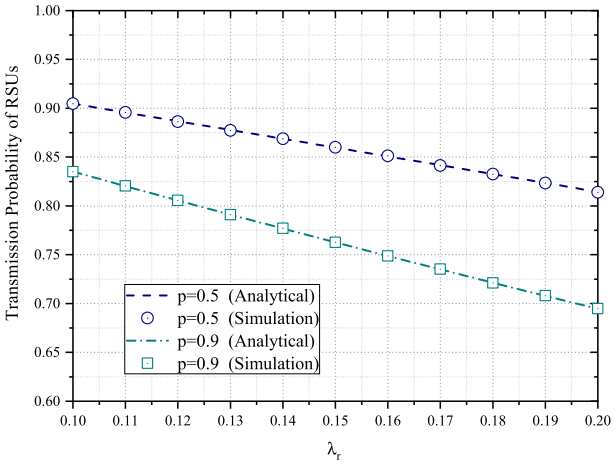

FIGURE 2. Transmission probability ς_r^a versus the density of RSUs λ_r.

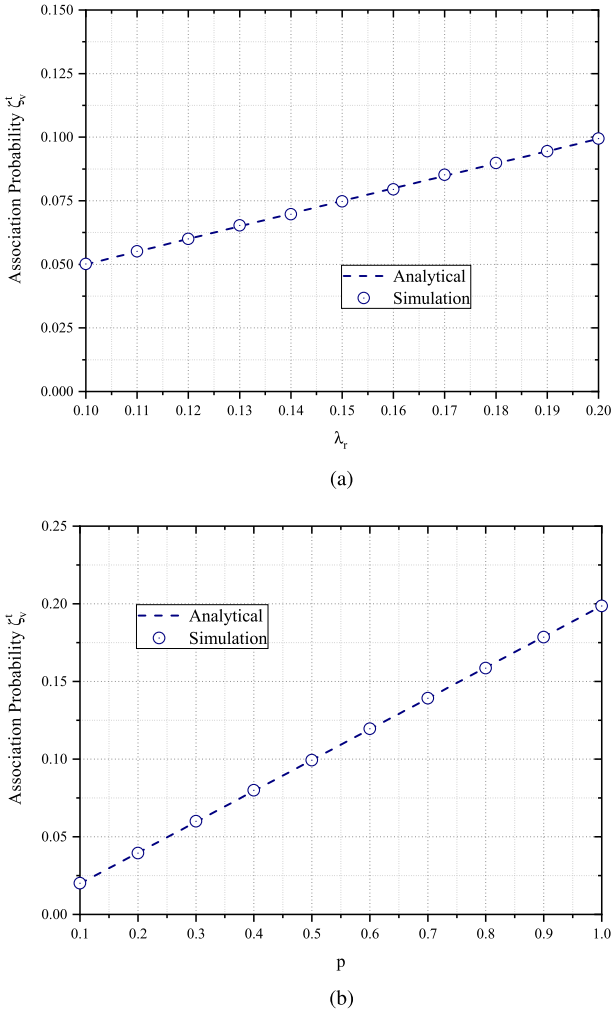

FIGURE 3. Association probability ζ_v^t versus the density of RSUs λ_r and the task occurrence probability p.

is set to be $P_v = 2$W. The bandwidth is set to be 1 MHz. The SIR target at vehicle receivers which associate with the paired transmitters for URLLC traffic is set as $\theta = 1$, and the data rate target at vehicle receivers which associate with

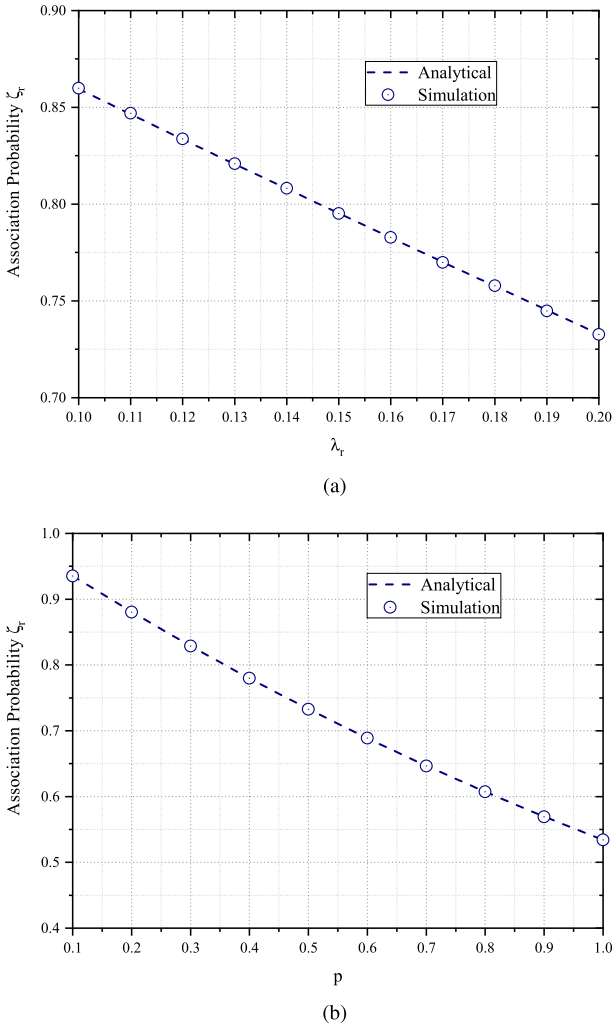

FIGURE 4. Association probability ζ_r versus the density of RSUs λ_r and the task occurrence probability p.

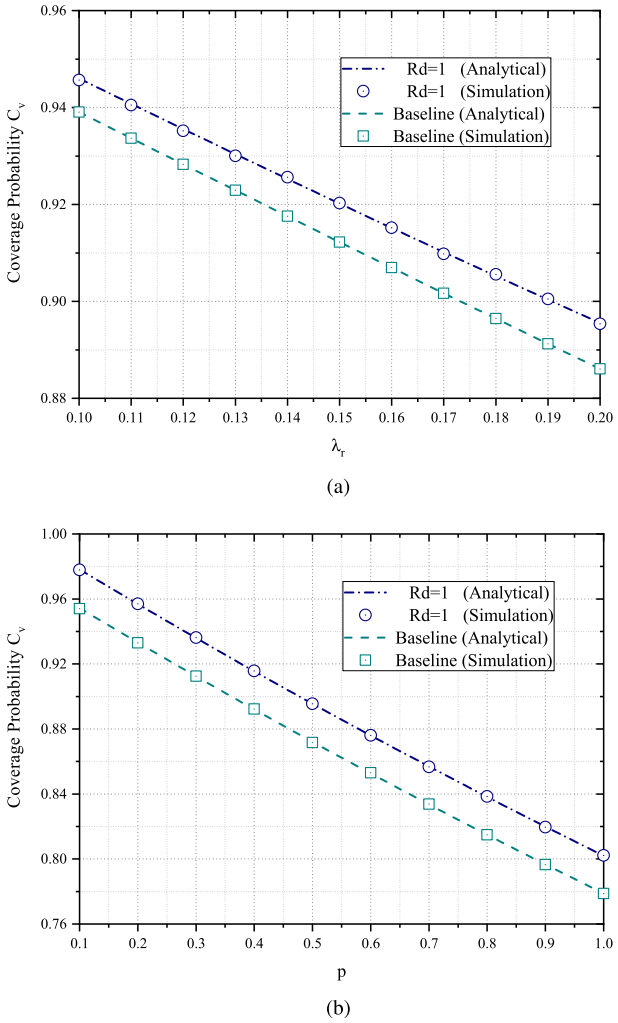

FIGURE 5. Coverage probability $\mathcal{C}_v$ versus the density of RSUs λ_r and the task occurrence probability p.

the RSU nodes for eMBB traffic is set as $\mathcal{T} = 0.1$. Further, the path loss exponent is set as $\alpha = 4$. The distance between vehicle receivers and their paired vehicle transmitters is set as $d_v = 0.5$, and the radius of guard zone is set as $R_d = 1$.

As illustrated in Fig. 2, the simulation results of the activation probability ς_r^a confirm the analytical values. Further, it can be observed from Fig. 2 that ς_r^a decreases with λ_r and p, which is coincides with our analysis. Particularly, this is mainly due to the fact that the increment of RSU nodes lead to the decrement of the mean load of RSU nodes, and thereby a degrade of the transmission probability.

Fig. 3 and 4 demonstrate the trends of ζ_v^t and ζ_r versus the density λ_r of RSUs and the arrival probability p of the URLLC traffic. It is shown that the theoretical estimates and simulating results of ζ_v^t and ζ_r are both consistent. It is also shown that ζ_v^t is an increasing function of λ_r and p. Intuitively, this is because that as λ_r or p increases, there is more likely for vehicle transmitters to be selected for URLLC transmission. On the other hand, different from ζ_{vt}, ζ_r is a decreasing function of λ_r and p, which is intuitively expected.

Fig. 5 plots the coverage probability $\mathcal{C}_v$ versus the density λ_r of RSUs and p. The analytical results are demonstrated to be accurate. Further, it is shown that $\mathcal{C}_v$ is a decreasing function of λ_r and p. Intuitively, this is because that as λ_r or p increase, the total interference increases, which thus deteriorates the coverage performance. In Fig. 5, we also compare the proposed guard-zone based URLLC scheduling policy with the baseline strategy where the guard zones around vehicle receivers are not applied. It is shown through Fig. 5 that the proposed guard-zone based URLLC scheduling policy achieves a better performance, which is due to the fact that the transmissions of the URLLC traffics is well protected by the guard zones.

Fig. 6 shows the analytical and simulated results of the rate coverage probability $\mathcal{C}_r$ versus the density λ_r of RSUs and p. It is shown that the analytical results are well consistent with the simulation results. Further, it is shown that $\mathcal{C}_r$ is an increasing function of λ_r, which is mainly due to the decrement of the mean load of a RSU as λ_r increases. It is also shown that $\mathcal{C}_r$ is an decreasing function of p, and this is due to the increment of the interference induced by the

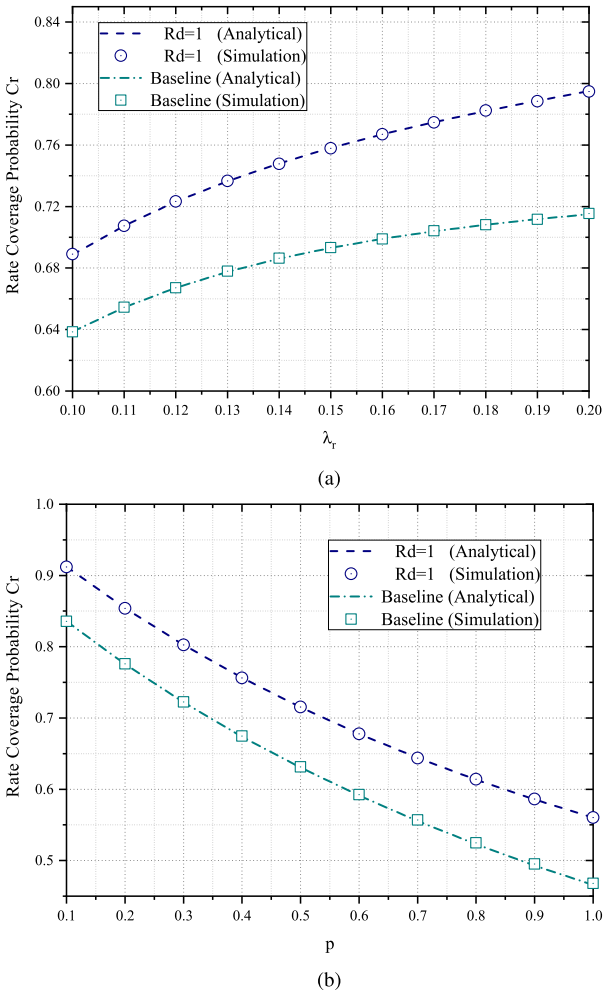

FIGURE 6. Rate coverage probability $\mathcal{C}_r$ versus the density of RSUs λ_r and the task occurrence probability p.

active vehicle transmitters. We further compare the rate coverage performance of the proposed guard-zone based URLLC scheduling policy with the baseline strategy where the guard zones around vehicle receivers are not applied. Notice that under the proposed guard-zone based URLLC scheduling policy, the load of the active RSU nodes is statistically smaller than that under the baseline strategy. As such, the proposed guard-zone based URLLC scheduling policy outperforms the baseline strategy on the rate coverage performance $\mathcal{C}_r$.

VI. CONCLUSION

In this paper, under the scenario of a one-way highway vehicular network, we addressed the issue of joint resource allocations of the eMBB and URLLC traffics for the enhancement of the network performance. The eMBB traffic is assumed to be full-buffered and scheduled at the boundary of each time slot for multimedia transmissions. During each eMBB transmission interval, random arrivals of URLLC traffics are assumed. To satisfy the latency constraint of the URLLC transmissions, the eMBB time slot is divided into minislots and the newly arrived URLLC traffic is promptly scheduled in the next minislot by puncturing the on-going eMBB traffics. Further, to guarantee the reliability of the URLLC traffic, guard zones are deployed around the vehicle receivers as protections and the eMBB transmissions inside the guard zones are prohibited. Under this context, we first derived the transmission probability of the RSU nodes. Then, based on the obtained results, we captured association probabilities of the vehicle receivers for URLLC and eMBB traffics, respectively. Finally, the coverage performance of the vehicle-to-vehicle (V2V) links and the rate coverage performance of the vehicle-to-infrastructure (V2I) links were analyzed. We confirmed our analysis and discussed the impact of the key network parameters on the joint scheduling of the URLLC and eMBB traffics through extensive simulations. We also compared the proposed guard-zone based URLLC scheduling policy with the baseline policy where the guard zone around vehicle receiver is not applied, and demonstrated the superiority.

APPENDIX A
PROOF OF THEOREM 4

Under the proposed guard-zone based URLLC scheduling policy, the received SIR of a vehicle receiver at location x in which associates with its paired vehicle transmitter for URLLC traffic is given by

$$\mathrm{SIR}_v = \frac{P_v g_v d_v^{-\alpha}}{\sum\limits_{i\in\Pi_r^t} P_r h_i |X_i - x|^{-\alpha} + \sum\limits_{i\in\Pi_v^a} P_v g_j |Y_j - x|^{-\alpha}} \tag{20}$$

where Π_r^t denotes the set of active RSU nodes, Π_v^a denotes the set of active vehicle transmitters, X_i is the location of the i-th active RSU, Y_j is the location of the j-th active vehicle transmitter, g_v denotes the power coefficient of the fading channel of the typical V2V link, h_i is the power coefficient of the fading channel between X_i and x, g_j is the power coefficient of the fading channel between Y_j and x, and $|X_i - x|$ and $|Y_j - x|$ denote the corresponding distance.

Then, we derive the coverage probability $\mathcal{C}_v$ as in (21), as shown at the top of the next page, where the probability density function of d_r is given by

$$f_d(d_r) = 2\lambda_r^a e^{-2\lambda_r^a d_r}.$$

Based on (21), we thus have

$$\begin{aligned}\mathcal{C}_v = \exp\Bigg\{ &-2\int_0^{R_d}\int_{R_d}^{\infty} 2\Big(\lambda_r(1-e^{-\frac{\lambda_v}{\lambda_r}})e^{-2\lambda_v^a R_d}\Big)^2 \\ &\times \frac{e^{-2\lambda_r(1-e^{-\frac{\lambda_v}{\lambda_r}})e^{-2\lambda_v^a R_d} d_r}}{1+\frac{P_v u^\alpha}{\theta P_r {d_v}^\alpha}} \cdot \mathrm{d}u\mathrm{d}d_r\Bigg\} \\ \times \exp\Bigg\{ &-2\int_{R_d}^{\infty}\int_{d_r}^{\infty} 2\Big(\lambda_r(1-e^{-\frac{\lambda_v}{\lambda_r}})e^{-2\lambda_v^a R_d}\Big)^2 \\ &\times \frac{e^{-2\lambda_r(1-e^{-\frac{\lambda_v}{\lambda_r}})e^{-2\lambda_v^a R_d} d_r}}{1+\frac{P_v u^\alpha}{\theta P_r {d_v}^\alpha}} \cdot \mathrm{d}u\mathrm{d}d_r\Bigg\} \\ \times \exp\Bigg\{ &-2\int_0^{\infty} \frac{\lambda_r p(1-e^{-\frac{\lambda_v}{\lambda_r}})}{1+\frac{u^\alpha}{\theta {d_v}^\alpha}}\mathrm{d}u\Bigg\} \\ = \exp\Bigg\{ &-2\Big(\eta + \int_{R_d}^{\infty} \varpi(d_r)\mathrm{d}d_r + \varrho\Big)\Bigg\}, \end{aligned} \tag{22}$$

$$
\begin{aligned}
\mathcal{C}_v &= \Pr\left\{\mathrm{SIR}_v > \theta\right\} \\
&= \Pr\left\{\frac{P_v g_v d_v^{-\alpha}}{\sum\limits_{i\in\Pi_r^t} P_r h_i |X_i|^{-\alpha} + \sum\limits_{j\in\Pi_v^a} P_v g_j |Y_j|^{-\alpha}} > \theta\right\} \\
&= \mathbb{E}_X\left[\prod_{i\in\Pi_r^t} \mathbb{E}_h\left[e^{-\frac{\theta P_r h_i |X_i|^{-\alpha}}{P_v d_v^{-\alpha}}}\right]\right] \cdot \mathbb{E}_Y\left[\prod_{j\in\Pi_v^a} \mathbb{E}_g\left[e^{-\frac{\theta P_v g_j |Y_j|^{-\alpha}}{P_v d_v^{-\alpha}}}\right]\right] \\
&= \exp\left\{-2\int_{\max\{d_r,R_d\}}^{\infty}\left(1-\int_0^{\infty} e^{-(\frac{\theta P_r u^{-\alpha}}{P_v d_v^{-\alpha}}+1)h}\mathrm{d}h\right)\lambda_r^a \mathrm{d}u\right\} \\
&\quad \times \exp\left\{-2\int_0^{\infty}\left(1-\int_0^{\infty} e^{-(\frac{\theta u^{-\alpha}}{d_v^{-\alpha}}+1)g}\mathrm{d}g\right)\lambda_v^a \mathrm{d}u\right\} \\
&= \exp\left\{-2\int_0^{R_d}\int_{R_d}^{\infty}\left(1-\int_0^{\infty} e^{-(\frac{\theta P_r u^{-\alpha}}{P_v d_v^{-\alpha}}+1)h}\mathrm{d}h\right)\lambda_r^a \mathrm{d}u f_d(d_r)\mathrm{d}d_r\right\} \\
&\quad \times \exp\left\{-2\int_{R_d}^{\infty}\int_{d_r}^{\infty}\left(1-\int_0^{\infty} e^{-(\frac{\theta P_r u^{-\alpha}}{P_v d_v^{-\alpha}}+1)h}\mathrm{d}h\right)\lambda_r^a \mathrm{d}u f_d(d_r)\mathrm{d}d_r\right\} \\
&\quad \times \exp\left\{-2\int_0^{\infty}\left(1-\int_0^{\infty} e^{-(\frac{\theta u^{-\alpha}}{d_v^{-\alpha}}+1)g}\mathrm{d}g\right)\lambda_v^a \mathrm{d}u\right\} \\
&= \exp\left\{-2\int_0^{R_d}\int_{R_d}^{\infty}\frac{\lambda_r^a \cdot f_d(d_r)}{1+\frac{P_v u^{\alpha}}{\theta P_r d_v^{\alpha}}}\mathrm{d}u\mathrm{d}d_r\right\} \\
&\quad \times \exp\left\{-2\int_{R_d}^{\infty}\int_{d_r}^{\infty}\frac{\lambda_r^a \cdot f_d(d_r)}{1+\frac{P_v u^{\alpha}}{\theta P_r d_v^{\alpha}}}\mathrm{d}u\mathrm{d}d_r\right\} \cdot \exp\left\{-2\int_0^{\infty}\frac{\lambda_v^a}{1+\frac{u^{\alpha}}{\theta d_v^{\alpha}}}\mathrm{d}u\right\}, \qquad (21)
\end{aligned}
$$

where η, $\varpi(d_r)$, and ϱ are given by

$$
\begin{aligned}
\eta = {} & \frac{\theta P_r {d_v}^{\alpha}}{(-1+\alpha)P_v}\left(1-e^{-\frac{\lambda_v}{\lambda_r}}\right) \\
& \times (1-e^{-2R_d\lambda_r(1-e^{-\frac{\lambda_v}{\lambda_r}})e^{-2\lambda_r(1-e^{-\frac{\lambda_v}{\lambda_r}})pR_d}}) \\
& \times e^{-2R_d\lambda_r(1-e^{-\frac{\lambda_v}{\lambda_r}})p}{\lambda_r}{R_d}^{1-\alpha} \\
& \times {}_2\mathrm{F}_1\left[1, \frac{-1+\alpha}{\alpha}, 2-\frac{1}{\alpha}, -\frac{\theta P_r\left(\frac{d_v}{R_d}\right)^{\alpha}}{P_v}\right], \qquad (23)
\end{aligned}
$$

$$
\begin{aligned}
\varpi(d_r) = {} & \frac{P_r\theta {d_r}^{1-\alpha}}{(-1+\alpha)P_v}\left(1-e^{-\frac{\lambda_v}{\lambda_r}}\right)^2 {d_v}^{\alpha} \\
& \times e^{-2(\lambda_r(1-e^{-\frac{\lambda_v}{\lambda_r}})e^{-2\lambda_r(1-e^{-\frac{\lambda_v}{\lambda_r}})pR_d}d_r)} \\
& \times 2\, e^{-4\lambda_r(1-e^{-\frac{\lambda_v}{\lambda_r}})pR_d}\ {\lambda_r}^2 \\
& \times {}_2\mathrm{F}_1\left[1, \frac{-1+\alpha}{\alpha}, 2-\frac{1}{\alpha}, -\frac{\theta P_r\left(\frac{d_v}{d_r}\right)^{\alpha}}{P_v}\right], \qquad (24)
\end{aligned}
$$

and

$$
\varrho = \frac{\left(1-e^{-\frac{\lambda_v}{\lambda_r}}\right)\lambda_r p\pi d_v \theta^{\frac{1}{\alpha}}\csc\left(\frac{\pi}{\alpha}\right)}{\alpha}, \qquad (25)
$$

respectively, with d_r denoting the distance between the tagged vehicle receiver and its nearest active RSU, and ${}_2\mathrm{F}_1(a, b; c; z)$ is defined by (13). This thus completes the proof.

APPENDIX B
PROOF OF LEMMA 1

Under the proposed guard-zone based URLLC scheduling policy, the received SIR of a vehicle receiver at location x which associates with its nearest RSU at location Y for eMBB traffic is given by

$$
\mathrm{SIR}_r = \frac{P_r h_r d^{-\alpha}}{\sum\limits_{i\in\Pi_r^t/\{Y\}} P_r h_i |X_i - x|^{-\alpha} + \sum\limits_{i\in\Pi_v^a} P_v g_j |Y_j - x|^{-\alpha}}, \qquad (26)
$$

where $d = |Y - x|$, Π_r^t denotes the set of active RSU nodes, Π_v^a denotes the set of active vehicle transmitters, X_i is the location of the i-th active RSU, Y_j is the location of the j-th active vehicle transmitter, h_r denotes the power coefficient of the fading channel of the typical V2I link, h_i is the power coefficient of the fading channel between X_i and x, g_j is the power coefficient of the fading channel between Y_j and x, and $|X_i - x|$ and $|Y_j - x|$ denote the corresponding distance. Then, we derive the coverage probability $\mathcal{C}_v$ as in (27), as shown at the top of the next page, where the probability density function of l_r is given by

$$
f_{l_r}(l) = 4\lambda_r^a l e^{-2\lambda_r^a l}.
$$

As such, based on (27), we have

$$
\mathcal{C}_d^r = \mathbb{E}_K\left[\exp\left\{-2\int_0^{2R_d}\int_{R_d}^{\infty}(\lambda_r(1-e^{-\frac{\lambda_v}{\lambda_r}})e^{-2\lambda_v^a R_d}\right)^2\right.
$$

$$
\begin{aligned}
\mathcal{C}_d^r &= \Pr\left\{\mathrm{SIR}_d^r > 2^{\frac{\mathcal{T}(K+1)}{W}} - 1\right\} \\
&= \Pr\left\{\frac{P_r h_r d^{-\alpha}}{\sum\limits_{i\in\Pi_r^l/\{Y\}} P_r h_i |X_i|^{-\alpha} + \sum\limits_{j\in\Pi_v^a} P_v g_j |Y_j|^{-\alpha}} > 2^{\frac{\mathcal{T}(K+1)}{W}} - 1\right\} \\
&= \mathbb{E}_X\left[\prod_{i\in\Pi_r^l}\mathbb{E}_h\left[e^{-\frac{(2^{\frac{\mathcal{T}(K+1)}{W}}-1)h_i|X_i|^{-\alpha}}{d^{-\alpha}}}\right]\right]\cdot\mathbb{E}_Y\left[\prod_{j\in\Pi_v^a}\mathbb{E}_g\left[e^{-\frac{(2^{\frac{\mathcal{T}(K+1)}{W}}-1)P_v g_j|Y_j|^{-\alpha}}{P_r d^{-\alpha}}}\right]\right] \\
&= \mathbb{E}_K\left[\exp\left\{-2\int_{\max\{\frac{l}{2},R_d\}}^{\infty}\left(1-\int_0^{\infty} e^{-(\frac{(2^{\frac{\mathcal{T}(K+1)}{W}}-1)u^{-\alpha}}{d^{-\alpha}}+1)h}\mathrm{d}h\right)\lambda_r^a \mathrm{d}u\right\}\right] \\
&\quad\times\mathbb{E}_K\left[\exp\left\{-2\int_0^{\infty}\left(1-\int_0^{\infty} e^{-(\frac{(2^{\frac{\mathcal{T}(K+1)}{W}}-1)P_v u^{-\alpha}}{P_r d^{-\alpha}}+1)g}\mathrm{d}g\right)\lambda_v^a \mathrm{d}u\right\}\right] \\
&= \mathbb{E}_K\left[\exp\left\{-2\int_0^{2R_d}\int_{R_d}^{\infty}\left(1-\int_0^{\infty} e^{-(\frac{(2^{\frac{\mathcal{T}(K+1)}{W}}-1)u^{-\alpha}}{d^{-\alpha}}+1)h}\mathrm{d}h\right)\lambda_r^a \mathrm{d}u f_{l_r}(l)\mathrm{d}l\right\}\right] \\
&\quad\times\mathbb{E}_K\left[\exp\left\{-2\int_{2R_d}^{\infty}\int_{\frac{l}{2}}^{\infty}\left(1-\int_0^{\infty} e^{-(\frac{(2^{\frac{\mathcal{T}(K+1)}{W}}-1)u^{-\alpha}}{d^{-\alpha}}+1)h}\mathrm{d}h\right)\lambda_r^a \mathrm{d}u f_{l_r}(l)\mathrm{d}l\right\}\right] \\
&\quad\times\mathbb{E}_K\left[\exp\left\{-2\int_0^{\infty}\left(1-\int_0^{\infty} e^{-(\frac{(2^{\frac{\mathcal{T}(K+1)}{W}}-1)P_v u^{-\alpha}}{P_r d^{-\alpha}}+1)g}\mathrm{d}g\right)\lambda_v^a \mathrm{d}u\right\}\right] \\
&= \mathbb{E}_K\left[\exp\left\{-2\int_0^{2R_d}\int_{R_d}^{\infty}\frac{\lambda_r^a\cdot f_{l_r}(l)}{1+\frac{u^{\alpha}}{(2^{\frac{\mathcal{T}(K+1)}{W}}-1)d^{\alpha}}}\mathrm{d}u\mathrm{d}l\right\}\right]\cdot\mathbb{E}_K\left[\exp\left\{-2\int_{2R_d}^{\infty}\int_{\frac{l}{2}}^{\infty}\frac{\lambda_r^a\cdot f_{l_r}(l)}{1+\frac{u^{\alpha}}{(2^{\frac{\mathcal{T}(K+1)}{W}}-1)d^{\alpha}}}\mathrm{d}u\mathrm{d}l\right\}\right] \\
&\quad\times\mathbb{E}_K\left[\exp\left\{-2\int_0^{\infty}\frac{\lambda_v^a}{1+\frac{P_r u^{\alpha}}{(2^{\frac{\mathcal{T}(K+1)}{W}}-1)P_v d^{\alpha}}}\mathrm{d}u\right\}\right], \qquad (27)
\end{aligned}
$$

$$
\begin{aligned}
&\times\frac{e^{-2\lambda_r(1-e^{-\frac{\lambda_v}{\lambda_r}})e^{-2\lambda_v^a R_d}l}}{1+\frac{u^{\alpha}}{(2^{\frac{\mathcal{T}(K+1)}{W}}-1)d^{\alpha}}}\cdot 4l\mathrm{d}u\mathrm{d}l\Bigg\}\Bigg] \\
&\times\mathbb{E}_K\left[\exp\left\{-2\int_{2R_d}^{\infty}\int_{\frac{l}{2}}^{\infty}(\lambda_r(1-e^{-\frac{\lambda_v}{\lambda_r}})e^{-2\lambda_v^a R_d}\right)^2\right. \\
&\times\left.\frac{e^{-2\lambda_r(1-e^{-\frac{\lambda_v}{\lambda_r}})e^{-2\lambda_v^a R_d}l}}{1+\frac{u^{\alpha}}{(2^{\frac{\mathcal{T}(K+1)}{W}}-1)d^{\alpha}}}\cdot 4\,l\mathrm{d}u\mathrm{d}l\right\}\Bigg] \\
&\times\mathbb{E}_K\left[\exp\left\{-2\int_0^{\infty}\frac{\lambda_r p(1-e^{-\frac{\lambda_v}{\lambda_r}})}{1+\frac{P_r u^{\alpha}}{(2^{\frac{\mathcal{T}(K+1)}{W}}-1)P_v d^{\alpha}}}\mathrm{d}u\right\}\right] \\
&= \sum_{k=0}^{\infty}\exp\left\{-2\left(\xi+\int_{2R_d}^{\infty}\varphi(l)\mathrm{d}l+\vartheta\right)\right\}\frac{(\frac{\lambda_v}{\lambda_r})^k}{k!}, \qquad (28)
\end{aligned}
$$

where K denote the random load in the tagged Voronoi cell of Y, and ξ, $\varphi(l)$, ϑ are given by

$$
\begin{aligned}
\xi &= -\frac{\left(-1+2^{\frac{\mathcal{T}(K+1)}{W}}\right)}{(-1+\alpha)}e^{-4\,R_d\lambda_r(1-e^{-\frac{\lambda_v}{\lambda_r}})e^{-2\lambda_r(1-e^{-\frac{\lambda_v}{\lambda_r}})pR_d} \\
&\quad\times\left(1-e^{4\,R_d\lambda_r(1-e^{-\frac{\lambda_v}{\lambda_r}})e^{-2\lambda_r(1-e^{-\frac{\lambda_v}{\lambda_r}})pR_d}}\right. \\
&\quad\left.+4\,R_d\lambda_r(1-e^{-\frac{\lambda_v}{\lambda_r}})e^{-2\lambda_r(1-e^{-\frac{\lambda_v}{\lambda_r}})pR_d}\right)\left(\frac{d}{R_d}\right)^{\alpha}R_d \\
&\quad\times{}_2\mathrm{F}_1\left[1,\frac{-1+\alpha}{\alpha},2-\frac{1}{\alpha},\left(1-2^{\frac{\mathcal{T}(K+1)}{W}}\right)\left(\frac{d}{R_d}\right)^{\alpha}\right], \qquad (29)
\end{aligned}
$$

$$
\begin{aligned}
\varphi(l) &= \frac{2^{\alpha+1}\left(-1+2^{\frac{\mathcal{T}(K+1)}{W}}\right)}{(-1+\alpha)}d^{\alpha}l^{2-\alpha} \\
&\quad\times\left(\lambda_r(1-e^{-\frac{\lambda_v}{\lambda_r}})\cdot e^{-2\lambda_r(1-e^{-\frac{\lambda_v}{\lambda_r}})pR_d}\right)^2 \\
&\quad\times{}_2\mathrm{F}_1\left[1,\frac{-1+\alpha}{\alpha},2-\frac{1}{\alpha},\left(1-2^{\frac{\mathcal{T}(K+1)}{W}}\right)\left(\frac{2d}{l}\right)^{\alpha}\right] \\
&\quad\times e^{-2l\lambda_r(1-e^{-\frac{\lambda_v}{\lambda_r}})\cdot e^{-2\lambda_r(1-e^{-\frac{\lambda_v}{\lambda_r}})pR_d}}, \qquad (30)
\end{aligned}
$$

and

$$
\vartheta = \lambda_r\left(1-e^{-\frac{\lambda_v}{\lambda_r}}\right)p\pi\left(\frac{d^{-\alpha}P_v}{\left(-1+2^{\frac{\mathcal{T}(K+1)}{W}}\right)P_r}\right)^{-\frac{1}{\alpha}}\frac{\csc(\frac{\pi}{\alpha})}{\alpha}, \qquad (31)
$$

respectively, with l denoting the size of active Voronoi cell. This thus completes the proof.

REFERENCES

[1] S. Biswas, R. Tatchikou, and F. Dion, "Vehicle-to-vehicle wireless communication protocols for enhancing highway traffic safety," *IEEE Commun. Mag.*, vol. 44, no. 1, pp. 74–82, Jan. 2006.

[2] H. Hartenstein and L. P. Laberteaux, "A tutorial survey on vehicular ad hoc networks," *IEEE Commun. Mag.*, vol. 46, no. 6, pp. 164–171, Jun. 2008.

[3] K. Guan, D. He, B. Ai, D. W. Matolak, Q. Wang, Z. Zhong, and T. Kürner, "5-GHz obstructed vehicle-to-vehicle channel characterization for Internet of intelligent vehicles," *IEEE Internet Things J.*, vol. 6, no. 1, pp. 100–110, Feb. 2019.

[4] B. Ai, K. Guan, M. Rupp, T. Kurner, X. Cheng, X.-F. Yin, Q. Wang, G.-Y. Ma, Y. Li, L. Xiong, and J.-W. Ding, "Future railway services-oriented mobile communications network," *IEEE Commun. Mag.*, vol. 53, no. 10, pp. 78–85, Oct. 2015.

[5] B. Ai, X. Cheng, T. Kürner, Z.-D. Zhong, K. Guan, R.-S. He, L. Xiong, D. W. Matolak, D. G. Michelson, and C. Briso-Rodriguez, "Challenges toward wireless communications for high-speed railway," *IEEE Trans. Intell. Transp. Syst.*, vol. 15, no. 5, pp. 2143–2158, Oct. 2014.

[6] R. He, B. Ai, G. Wang, K. Guan, Z. Zhong, A. F. Molisch, C. Briso-Rodriguez, and C. P. Oestges, "High-speed railway communications: From GSM-R to LTE-R," *IEEE Veh. Technol. Mag.*, vol. 11, no. 3, pp. 49–58, Sep. 2016.

[7] L. Liang, H. Peng, G. Y. Li, and X. Shen, "Vehicular communications: A physical layer perspective," *IEEE Trans. Veh. Technol.*, vol. 66, no. 12, pp. 10647–10659, Dec. 2017.

[8] Y. Zhang, H. Zhang, K. Long, Q. Zheng, and X. Xie, "Software-defined and fog-computing-based next generation vehicular networks," *IEEE Commun. Mag.*, vol. 56, no. 9, pp. 34–41, Sep. 2018.

[9] P. Dai, K. Liu, L. Feng, H. Zhang, V. C. S. Lee, S. H. Son, and X. Wu, "Temporal information services in large-scale vehicular networks through evolutionary multi-objective optimization," *IEEE Trans. Intell. Transp. Syst.*, vol. 20, no. 1, pp. 218–231, Jan. 2019.

[10] Q. Zheng, K. Zheng, H. Zhang, and V. C. M. Leung, "Delay-optimal virtualized radio resource scheduling in software-defined vehicular networks via stochastic learning," *IEEE Trans. Veh. Technol.*, vol. 65, no. 10, pp. 7857–7867, Oct. 2016.

[11] H. Peng, L. Liang, X. Shen, and G. Y. Li, "Vehicular communications: A network layer perspective," *IEEE Trans. Veh. Technol.*, vol. 68, no. 2, pp. 1064–1078, Feb. 2019.

[12] P. Papadimitratos, A. De La Fortelle, K. Evenssen, R. Brignolo, and S. Cosenza, "Vehicular communication systems: Enabling technologies, applications, and future outlook on intelligent transportation," *IEEE Commun. Mag.*, vol. 47, no. 11, pp. 84–95, Nov. 2009.

[13] *Technical Specification Group Radio Access Network; Study on LTE-Based V2X Services; (Release 14)*, document 3GPP TR 36.885 V14.0.0, Jun. 2016.

[14] *Technical Specification Group Radio Access Network; Study Enhancement 3GPP Support for 5G V2X Services; (Release 15)*, document 3GPP TR 22.886 V15.1.0, Mar. 2017.

[15] Z. Wu, F. Zhao, and X. Liu, "Signal space diversity aided dynamic multiplexing for eMBB and URLLC traffics," in *Proc. 3rd IEEE Int. Conf. Comput. Commun. (ICCC)*, Chengdu, China, Dec. 2017, pp. 1396–1400.

[16] A. Anand, G. De Veciana, and S. Shakkottai, "Joint scheduling of URLLC and eMBB traffic in 5G wireless networks," in *Proc. IEEE Conf. Comput. Commun. (INFOCOM)*, Honolulu, HI, USA, Apr. 2018, pp. 1970–1978.

[17] J. Park and M. Bennis, "URLLC-eMBB slicing to support VR multimodal perceptions over wireless cellular systems," in *Proc. IEEE Global Commun. Conf. (GLOBECOM)*, Abu Dhabi, UAE, Dec. 2018, pp. 1–7.

[18] R. Kassab, O. Simeone, and P. Popovski, "Coexistence of URLLC and eMBB services in the c-RAN uplink: An information-theoretic study," in *Proc. IEEE Global Commun. Conf. (GLOBECOM)*, Abu Dhabi, UAE, Dec. 2018, pp. 1–6.

[19] A. A. Esswie and K. I. Pedersen, "Null space based preemptive scheduling for joint URLLC and eMBB traffic in 5G networks," in *Proc. IEEE Globecom Workshops (GC Wkshps)*, Abu Dhabi, UAE, Dec. 2018, pp. 1–6.

[20] A. A. Esswie and K. I. Pedersen, "Capacity optimization of spatial preemptive scheduling for joint URLLC-eMBB traffic in 5G new radio," in *Proc. IEEE Globecom Workshops (GC Wkshps)*, Abu Dhabi, UAE, Dec. 2018, pp. 1–6.

[21] J. Tang, B. Shim, and T. Q. S. Quek, "Service multiplexing and revenue maximization in sliced C-RAN incorporated with URLLC and multicast eMBB," *IEEE J. Sel. Areas Commun.*, vol. 37, no. 4, pp. 881–895, Apr. 2019.

[22] J. Zhang, X. Xu, K. Zhang, B. Zhang, X. Tao, and P. Zhang, "Machine learning based flexible transmission time interval scheduling for eMBB and uRLLC coexistence scenario," *IEEE Access*, vol. 7, pp. 65811–65820, 2019.

[23] M. Alsenwi, N. H. Tran, M. Bennis, A. K. Bairagi, and C. S. Hong, "EMBB-URLLC resource slicing: A risk-sensitive approach," *IEEE Commun. Lett.*, vol. 23, no. 4, pp. 740–743, Apr. 2019.

[24] M. Alsenwi, S. R. Pandey, Y. K. Tun, K. T. Kim, and C. S. Hong, "A chance constrained based formulation for dynamic multiplexing of eMBB-URLLC traffics in 5G new radio," in *Proc. Int. Conf. Inf. Netw. (ICOIN)*, Kuala Lumpur, Malaysia, Jan. 2019, pp. 108–113.

[25] A. Karimi, K. I. Pedersen, N. H. Mahmood, G. Pocovi, and P. Mogensen, "Efficient low complexity packet scheduling algorithm for mixed URLLC and eMBB traffic in 5G," in *Proc. IEEE 89th Veh. Technol. Conf. (VTC-Spring)*, Kuala Lumpur, Malaysia, Apr./May 2019, pp. 1–6.

[26] J.-S. Ferenc and Z. Néda, "On the size distribution of Poisson Voronoi cells," *Phys. A, Stat. Mech. Appl.*, vol. 385, no. 2, pp. 518–526, 2007.

[27] B. Blaszczyszyn, P. Mühlethaler, and Y. Toor, "Maximizing throughput of linear vehicular ad-hoc networks (VANETs)—A stochastic approach," in *Proc. Eur. Wireless Conf.*, May 2009, pp. 32–36.

[28] M. J. Farooq, H. ElSawy, and M.-S. Alouini, "A stochastic geometry model for multi-hop highway vehicular communication," *IEEE Trans. Wireless Commun.*, vol. 15, no. 3, pp. 2276–2291, Mar. 2016.

[29] Y. Wang, K. Venugopal, R. W. Heath, Jr., and A. F. Molisch, "MmWave vehicle-to-infrastructure communication: Analysis of urban microcellular networks," *IEEE Trans. Veh. Technol.*, vol. 67, no. 8, pp. 7086–7100, Aug. 2018.

[30] V. V. Chetlur and H. S. Dhillon, "Success probability and area spectral efficiency of a VANET modeled as a Cox process," *IEEE Wireless Commun. Lett.*, vol. 7, no. 5, pp. 856–859, Oct. 2018.

[31] V. V. Chetlur and H. S. Dhillon, "Coverage and rate analysis of downlink cellular vehicle-to-everything (C-V2X) communication," Jan. 2019, *arXiv:1901.09236*. [Online]. Available: https://arxiv.org/abs/1901.09236

[32] C.-H. Lee and M. Haenggi, "Interference and outage in Poisson cognitive networks," *IEEE Trans. Wireless Commun.*, vol. 11, no. 4, pp. 1392–1401, Apr. 2012.

[33] X. Song, C. Yin, D. Liu, and R. Zhang, "Spatial throughput characterization in cognitive radio networks with threshold-based opportunistic spectrum access," *IEEE J. Sel. Areas Commun.*, vol. 32, no. 11, pp. 2190–2204, Nov. 2014.

[34] T. V. Nguyen and F. Baccelli, "A probabilistic model of carrier sensing based cognitive radio," in *Proc. IEEE Symp. New Frontiers Dyn. Spectr.*, Singapore, Apr. 2010, pp. 1–12.

[35] X. Song, X. Meng, X. Shen, and C. Jia, "Cognitive radio networks with primary receiver assisted interference avoidance protocol," *IEEE Access*, vol. 6, pp. 1224–1235, 2017.

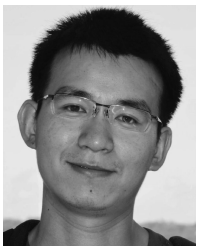

XIAOSHI SONG (S'08–M'14) received the B.E. degree in electrical engineering from the Dalian University of Technology, Dalian, China, in 2008, and the Ph.D. degree in information and communication engineering from the Beijing University of Posts and Telecommunications, Beijing, China, in 2014. He was a Visiting Ph.D. Student with the University of California, Irvine, USA, from 2011 to 2013, and a Visiting Scholar with The University of Hong Kong, Hong Kong, from July 2014 to October 2014. Since 2014, he has joined the School of Computer Science and Engineering of Northeastern University, Shenyang, China, as an Assistant Professor. His research interests include stochastic geometry and its applications in large-scale wireless networks, multiuser information theory, and wireless communication.

MENGYING YUAN is currently pursuing the bachelor's degree with the School of Computer Science and Engineering, Northeastern University, Shenyang, China. Her current research interests include stochastic geometry, queueing theory, and opportunistic spectrum design in fog-aided D2D networks.